ELSEVIER

Catalysis Today 39 (1997) 21–32

CATALYSIS TODAY

Hydrodesulfurization of dibenzothiophene derivatives over TiO_2–Al_2O_3 supported sulfided molybdenum catalyst

C. Pophal[b], F. Kameda[a], K. Hoshino[a], S. Yoshinaka[a], K. Segawa[a,*]

[a]*Department of Chemistry, Faculty of Science and Technology, Sophia University, 7-1 Kioi-cho, Chiyoda-ku, Tokyo 102, Japan*
[b]*Fachbereich Materialwissenschaft, Technische Hochschule Darmstadt, Petersenstr. 23, D-64287 Darmstadt, Germany*

Abstract

Composite TiO_2–Al_2O_3 supports with different loadings of TiO_2 have been prepared by chemical vapor deposition (CVD), using $TiCl_4$ as the precursor. The supports have been characterized by N_2 adsorption measurements, X-ray photoelectron spectroscopy (XPS), X-ray fluorescence analysis (XRF) and IR spectroscopy. The specific surface area of each TiO_2–Al_2O_3 support is comparable to that of γ-Al_2O_3. High dispersion of TiO_2 on the Al_2O_3 surface has been obtained, and no cluster formation has been detected. Mo/TiO_2–Al_2O_3 and Ni–Mo/TiO_2–Al_2O_3 catalysts have been synthesized by impregnation and co-impregnation method. We studied the conversion of Mo and Ni from the oxidic to the sulfidic state by XPS. Furthermore, the catalytic behavior of Mo and Ni–Mo supported on Al_2O_3, TiO_2 and TiO_2–Al_2O_3 has been investigated for the deep hydrodesulfurization (HDS) of dibenzothiophene (DBT) and methyl substituted DBT derivatives. The conversion over the TiO_2–Al_2O_3 supported catalysts, in particular for the HDS of 4-methyl-DBT (4-MDBT) and 4,6-dimethyl-DBT (4,6-DMDBT), is much higher than the conversion obtained over Al_2O_3 supported materials. In particular with regard to the Ni–Mo catalysts, the ratio of the corresponding cyclohexylbenzene (CHB)/biphenyl (BP) derivatives is increased over the composite support, indicating that the prehydrogenation of an aromatic ring is important for the HDS of DBT derivatives over TiO_2–Al_2O_3 supported catalysts. © 1997 Elsevier Science B.V.

Keywords: Ni–Mo catalysts; Hydrodesulfurization; Titania–alumina support; Chemical vapor deposition

1. Introduction

Recently, the interest in the deep hydrodesulfurization (HDS) (sulfur content <0.05 wt%) of gas oil has been renewed due to the stricter regulations concerning the sulfur content in diesel oil. In order to protect the global environment, the Japanese government has lowered the limit of the sulfur content to 0.05 wt% in 1997. To meet this assignment, the development of a suitable catalyst for the deep HDS is a very urgent subject. Because of cost requirements, reaction temperatures below 723 K and reaction pressures below 3.5 MPa are desirable. In the petrochemical industry, γ-alumina supported molybdenum oxide catalysts promoted with cobalt or nickel have been widely used for the HDS of sulfur compounds. They are as well used for other industrial processes such as hydrocracking of heavy crude oil fractions, oxidations of aliphatic alcohols, polymerization, metathesis, isomerization and hydrogenation of alkanes. Recently, TiO_2 supported molybdena catalysts have attracted increasing

*Corresponding author.

PII S0920-5861(97)00085-0

attention, because of their higher reducibility to a lower valence state of molybdenum and their higher catalytic activity for HDS [1–3], as well as for hydrocracking, compared to alumina supported materials [4]. Various studies focused on the characterization of molybdenum species supported on TiO_2, using several experimental techniques such as Raman spectroscopy, X-ray photoelectron spectroscopy (XPS) and temperature programmed reduction (TPR) [5–15]. The formation of the active sites when MoO_3 changes to MoS_2 by sulfurization has been elucidated by Arnoldy et al. [16]. Nishijima et al. [17] and Shimada et al. [18] have investigated molybdenum catalysts supported on Al_2O_3, TiO_2, SiO_2 and MgO by means of extended X-ray absorption fine structure (EXAFS), XPS and Raman spectroscopy. They reported the presence of different molybdenum species on the surface of the supports investigated. However, pure TiO_2 supports have very small specific surface areas compared to alumina, and it is difficult to make pellets. Furthermore, the active anatase structure possesses only low thermal stability. This makes TiO_2 support alone unsuitable for industrial applications. In order to overcome these drawbacks, increasing attention is being paid to the development of titania–alumina composite supports [19–25].

4-methyl-dibenzothiophene (4-MDBT) and 4,6-dimethyl-dibenzothiophene (4,6-DMDBT) are key sulfur compounds in the gas oil fraction and make Arabian light middle distillates difficult to desulfurize [26–31]. Nevertheless, in order to achieve deep HDS, it is essential to desulfurize these molecules. Two reaction pathways for the HDS of alkyl substituted dibenzothiophene (DBT) are proposed; they are illustrated in Scheme 1. The direct sulfur abstraction (direct desulfurization route) leads to BP derivatives, whereas prehydrogenation is forming hexahydrodibenzothiophene as an intermediate (HDS route), which is desulfurized to cyclohexylbenzene (CHB) derivatives. Furthermore, it is known that hydrogenation of neighboring phenyl groups reduces the steric hindrance caused by the methyl groups. Mochida and co-workers [32] presented the rate constants for the desulfurization step of the hydrogenated intermediates and compared them with the rate constants for the direct desulfurization. In the case of 4-MDBT, the rate constant for the desulfurization step of the hydrogenated intermediates was 30–35 times higher and 100

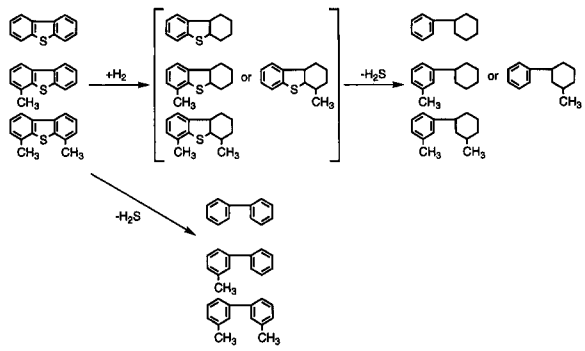

Scheme 1. Reaction pathways in HDS of DBT, 4-MDBT and 4,6-DMDBT.

times higher for 4,6-DMDBT, compared to the value obtained for direct desulfurization. Most recently Kabe and co-workers [33] reported the activation energies, the adsorption heat and the product selectivity for the deep HDS of DBT, 4-MDBT and 4,6-DMDBT over three commercially available Co–Mo/Al_2O_3 and one Ni–Mo/Al_2O_3 catalyst. The activity of the Ni-promoted molybdenum catalysts was higher than the activity of the Co-promoted materials. At higher temperatures, the formation of CHB derivatives from the biphenyl (BP) derivatives became important in the case of Ni–Mo/Al_2O_3. According to this publication, the rather low reactivities of 4-MDBT and 4,6-DMDBT were not attributed to the inhibition of adsorption, but to the steric hindrance in the C–S bond scission of the adsorbed molecules.

However, coating of the surface of commercially available γ-alumina with TiO_2 may lead to TiO_2–Al_2O_3 composite supports which could help to overcome the disadvantages of pure titania supports, as pointed out above. In the present work, we therefore focused on the preparation of TiO_2-coated alumina composite supports by chemical vapor deposition (CVD), using $TiCl_4$ as precursor and different loadings of TiO_2. To examine the catalytic activity of the TiO_2–Al_2O_3 supported Mo and Ni–Mo catalysts, we studied the deep HDS of DBT derivatives, such as 4-MDBT, 4,6-DMDBT, 2-methyl-DBT (2-MDBT) and 2,8-dimethyl-DBT (2,8-DMDBT), using mild reaction conditions. In our study, we compared the conversions for the HDS of DBT, 4-MDBT and 4,6-DMDBT over Mo/Al_2O_3, Mo/TiO_2, Mo/TiO_2–Al_2O_3 and the corresponding Ni-promoted catalysts.

To elucidate the influence of the positions of methyl-groups on the conversion rate, we studied the HDS of a mixture of DBT, 2-MDBT and 2,8-DMDBT, as well as of a mixture of DBT, 4-MDBT and 4,6-DMDBT over Ni–Mo catalysts on the different supports.

2. Experimental

2.1. Preparation

Titania (TiO_2) was supplied by Degussa (P-25, 51 $m^2 g^{-1}$) and the alumina (γ-Al_2O_3) support was provided by NIKKI (N611-N, 186 $m^2 g^{-1}$). The composite types of TiO_2–Al_2O_3 supports were prepared by CVD method of $TiCl_4$ on γ-alumina [34,35], according to the following procedure: 2 g of Al_2O_3 (12–24 mesh) substrate was placed in a quartz tubular reactor and pretreated for 2 h at 773 K in oxygen flow. The substrate was then exposed to $TiCl_4$ (WAKO) vapor (0.43 kPa) at 473 K, when $TiCl_4$ was mixed with N_2 as carrier gas. The deposition time was varied between 0.5 and 20 h, in order to obtain different loadings of TiO_2. Afterwards, the sample was hydrolyzed by water vapor (2.30 kPa) with N_2 as carrier gas at 473 K for 2 h. Calcination was carried out under O_2 flow for 2 h at 773 K. The supported molybdena catalysts used in this study were prepared by an impregnation method. Impregnation was performed at 323 K for 100 h, using an aqueous solution of ammonium heptamolybdate (0.004 M, WAKO). The supported Ni–Mo catalysts were prepared by co-impregnation, according to the pore filling method, using an aqueous solution of ammonium heptamolybdate (0.026 M) and nickel nitrate (0.695 M, WAKO). After impregnation, all materials were calcined at 773 K for 10 h in air.

2.2. Reaction conditions

The HDS reaction was carried out in a fixed bed high pressure flow reactor, consisting of a 0.5 in. stainless steel tube packed with 125–500 mg catalyst mixed with quartz sand. Before the reaction, the catalysts were dried at 773 K for 5 h under oxygen stream and presulfided with a mixture of H_2S (5%) and H_2 for 2 h at 573 K under atmospheric pressure. After purging of excess H_2S by nitrogen stream at 573 K for 0.5 h, H_2 and the reaction mixture were supplied to the reactor.

The used methyl-substituted DBT derivatives were synthesized as described in the literature [36]. All reaction mixtures used in this study were diluted in *n*-dodecane. The initial content of sulfur was 0.05 wt% and the reaction temperature was 573 K (H_2 pressure: 3 MPa, H_2 flow rate: 0.2 $dm^3 min^{-1}$, LHSV: 6.04–48.32 h^{-1}). The liquid products collected from a gas–liquid separator were analyzed by GC (Hitachi G-3000) and GC–MS (GC: Hewlett Packard 5890 Series II, MS: Nihondenshi JMS-SX 102A). The activity of the catalysts under investigation was estimated by the conversion of the DBT derivatives and by the ratio of the products after reaching steady state.

2.3. Characterization of the catalysts

IR measurements have been carried out in order to detect changes of the vibrational bands of hydroxyl groups on the surface of the alumina support caused by increased loading with TiO_2. Spectra were taken at room temperature on a Hitachi Model 270-30, in the range from 3900 to 3000 cm^{-1}. Before data collection, the samples were evacuated at 773 K for 2 h.

Nitrogen adsorption measurements were performed at 77 K on a Bel Japan Belsorp 28SA to determine the specific surface area. As pretreatment, 200 mg of support were placed in a quartz tube and evacuated for 6 h at 573 K. The pore volume and the pore size distribution was obtained by the Dollimore–Heal method [37].

XPS measurements were carried out at room temperature to investigate the state of molybdenum and nickel species on the surface of the different supports. Data were collected before and after sulfiding for 2 h at 573 K, with 5% H_2S diluted in H_2. The data were taken on a Surface Science Laboratory SSX-100 spectrometer, using monochromized Al Kα-radiation (1486.6 eV) and the C (1s) binding energy (285.0 eV) as reference. Before measuring, all samples have been evacuated and pretreated at 573 K. The X-ray fluorescence (XRF) measurements have been performed on a SXF-1200 analyzer from Shimadzu.

3. Results and discussion

3.1. Characterization of the supports

The IR spectra of γ-alumina and of TiO_2–Al_2O_3 composite supports with different loadings of TiO_2 are displayed in Fig. 1. Before CVD treatment, bands appear at 3762, 3723 and 3680 cm^{-1}. They correspond to hydroxyl stretching vibrations of Al–OH groups. The bands are rather broad, due to the fact that the alumina support is a poorly crystalline material. Even at low TiO_2 loadings (2.3 wt%), the vibrational band at 3762 cm^{-1} has almost disappeared. The bands at 3723 and 3680 cm^{-1} are not significantly affected at very low TiO_2 coverages. Nevertheless, a further increase of the TiO_2 loading, up to a total amount of 11 wt% leads to a strong decrease of the integral intensities of all observed vibrational bands. This implies the substitution of Al–OH groups on the surface of γ-alumina by Al–O–Ti bridges during the CVD process. Furthermore, the facts that almost all bands of Al–OH groups disappear, and that the decrease is directly correlated to the TiO_2 loading, indicate a high dispersion and coating of Ti-species on the Al_2O_3 surface by CVD.

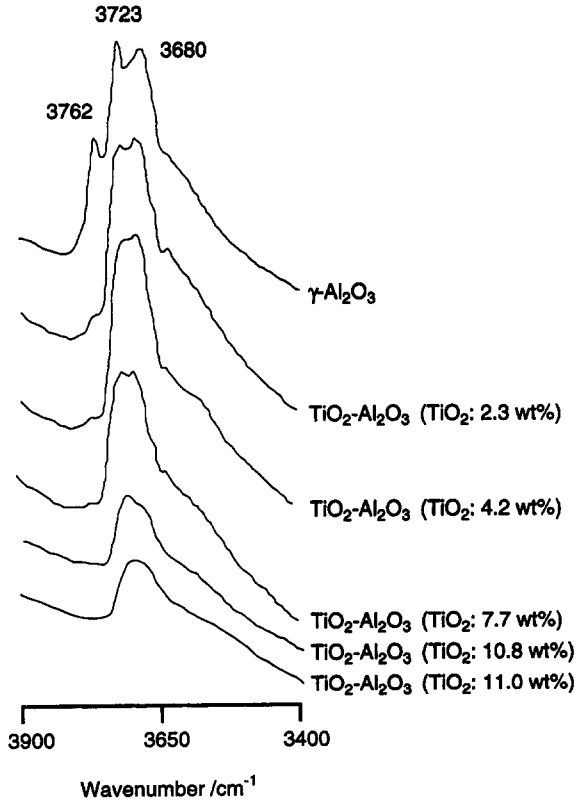

Fig. 1. IR spectra of γ-Al_2O_3 and composite TiO_2–Al_2O_3 supports with different TiO_2 loadings.

Table 1
Specific surface area and pore volume of γ-Al_2O_3, TiO_2 and composite TiO_2–Al_2O_3 support loaded with different amounts of titania

Deposition time (h)	TiO_2 (wt%)	Specific surface area ($m^2\ g^{-1}$)	Pore volume ($cm^3\ g^{-1}$)
0	—	186	0.44
0.5	2.53	182 (187)	0.42
4	4.86	177 (186)	0.41
8	6.64	174 (186)	0.40
12	8.94	168 (185)	0.36
16	11.15	162 (183)	0.37
20	13.69	154 (179)	0.35

Values in parentheses correspond to the specific surface area calculated for 1 g of Al_2O_3.

The results obtained by XRF and N_2 adsorption measurements for TiO_2–Al_2O_3 supports, prepared using different deposition times, are given in Table 1. XRF studies clearly reveal an increase of the TiO_2 loading with increasing deposition time. This leads to a decrease of the specific surface area of the TiO_2–Al_2O_3 supports from 186 $m^2\ g^{-1}$ for pure Al_2O_3 to 154 $m^2\ g^{-1}$ for the TiO_2–Al_2O_3 composite support loaded with 13.96 wt% TiO_2. However, the specific surface area calculated for 1 g of Al_2O_3 is not significantly affected. This linear decrease of the specific surface area of the composite support with increasing TiO_2 coverages reflects, in agreement with the IR studies, a high dispersion of titania. At TiO_2 loadings of 13.96 wt%, the surface area of the TiO_2–Al_2O_3 support is still three times larger than the specific surface area of the commercially available pure TiO_2 support. The pore volume is also decreased with increasing amount of TiO_2 covered on the γ-alumina support. Nevertheless, the decrease of the specific surface area and the pore volume is not very significant. A large specific surface area and a large pore volume is still preserved while coating the alumina support with TiO_2, using the CVD method.

Fig. 2 shows the pore size distribution obtained for γ-Al_2O_3, TiO_2 and TiO_2–Al_2O_3 composite supports

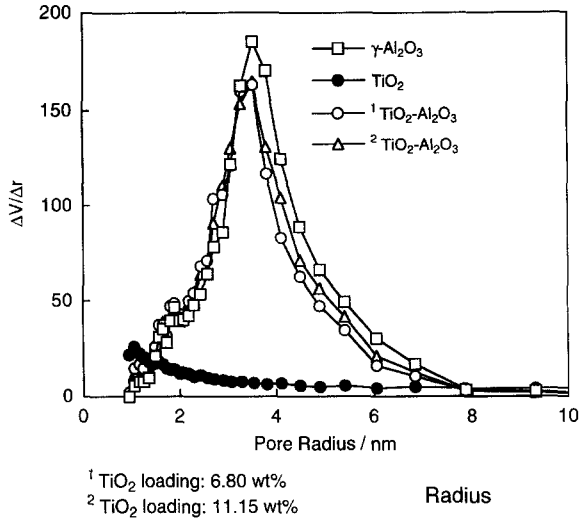

Fig. 2. Pore size distribution of different supports.

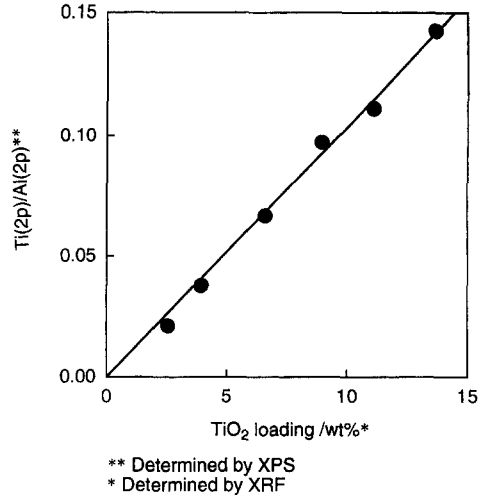

Fig. 3. Bulk and surface composition of TiO_2–Al_2O_3 supports prepared by CVD.

(6.80 wt% TiO_2 and 11.15 wt% TiO_2). From Fig. 2, it is obvious that pure TiO_2 possesses no pore system. With regard to γ-Al_2O_3 and TiO_2–Al_2O_3, the average pore diameter is only slightly shifted to lower values, whereas the distribution of the pore volume is not significantly affected by the coverage of alumina with TiO_2. These results reflect a homogeneous dispersion of TiO_2 on the surface of the Al_2O_3 support. The resulting composite TiO_2–Al_2O_3 support remains mesoporous, with a more or less monomodal pore size distribution and an average pore radius of about 3.8 nm. Significant discrepancies in the pore size distribution, caused by the different loadings of the two investigated TiO_2–Al_2O_3 support, have not been detected.

A comparison of the data obtained by XRF and XPS is depicted in Fig. 3. The increase of the total TiO_2 loading determined by XRF leads to a linear increase of TiO_2 amount on the surface, which was determined by means of XPS. Thus, TiO_2 can be assumed to be situated on the surface of the Al_2O_3 support, and the incorporation of significant amounts of titanium into the γ-alumina matrix can, within the sensitivity of the investigation methods, be excluded.

Judging by the results described above, we can assume that TiO_2 covers the surface of the γ-alumina support mainly without forming precipitations. The IR spectra described above strongly support this assumption, even though the vibrational bands of Al–OH groups are not completely eliminated at loadings of 11 wt% TiO_2. This might be due to the fact that the alumina surface is not completely covered. With regard to a closed packing of TiO_2 and under the assumptions of a titania monolayer, the specific area of the γ-alumina support would be completely covered at loadings of about 15 wt% titania. Furthermore, it is known that in the bulk phase of poorly crystalline alumina there are Al–OH groups present, even after calcination. These hydroxyl groups cannot be substituted by Al–O–Ti groups, and the corresponding vibrational bands in the IR spectra remain unchanged. Nevertheless, higher loadings of titania may lead to a more complete elimination of hydroxyl bands on the alumina surface. The comparison of the surface composition and the total amount of TiO_2 unambiguously reveals that TiO_2 is highly dispersed on the surface of the γ-alumina support. According to these results, CVD allows the coverage of the surface of alumina supports by TiO_2, using $TiCl_4$ as precursor without forming large aggregates, under variation of the TiO_2 loading over a wide range.

3.2. XPS studies

Molybdenum XPS investigations have been performed in order to elucidate the state of molybdenum sites on the TiO_2–Al_2O_3 support. The results obtained by the Mo 3d XPS spectra for calcined and sulfided

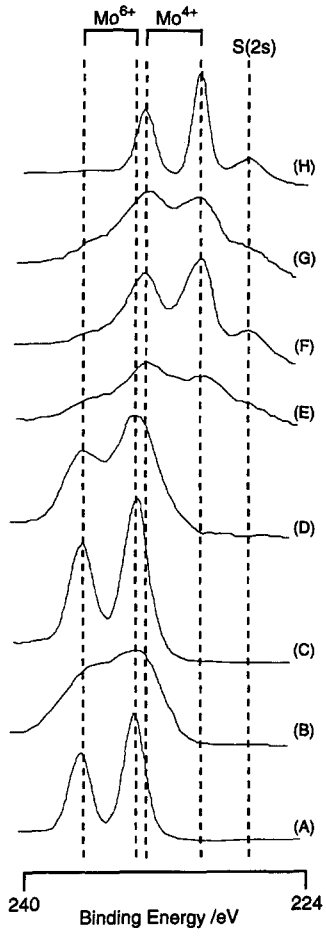

Fig. 4. Mo 3d XPS spectra of the calcined (A, B, C, D), the sulfided (E, F, G) materials and of crystalline MoS_2 (H): MoO_3 (A), Mo/Al_2O_3 (B, E), Mo/TiO_2 (C, F), Mo/TiO_2–Al_2O_3 (10.0 wt% TiO_2) (D, G).

Mo/Al_2O_3, Mo/TiO_2, Mo/TiO_2–Al_2O_3, crystalline MoO_3 and crystalline MoS_2 powder are illustrated in Fig. 4. The peaks obtained for Mo/Al_2O_3 (B) and Mo/TiO_2–Al_2O_3 (D) are much broader than those obtained for MoO_3 (A) and Mo/TiO_2 (C), whereas the binding energy distribution detected for Mo/Al_2O_3 (B) is broader than that of Mo/TiO_2–Al_2O_3 (D). Furthermore, the binding energies were strongly dependent on the support. The binding energies of crystalline MoO_3 are 236.5 and 233.5 eV, while the lowest binding energies have been obtained for Mo/Al_2O_3 (235.7 and 232.6 eV). However, the binding energies of the calcined materials increase in the following order: Mo/Al_2O_3<Mo/TiO_2–Al_2O_3<Mo/TiO_2. According to these differences, the support affects the average valence state of the molybdenum species. Metals possessing a higher oxidation state are generally assumed to experience higher binding energies [38,39]. Different interactions between the Mo-species and the supports are known to affect the value of the molybdenum binding energies. However, the specific surface areas of TiO_2–Al_2O_3 and γ-alumina are about three times higher than that of the TiO_2 support. The spectra of crystalline MoO_3 and Mo/TiO_2 are very similar, with regard to the binding energy as well as with regard to the full widths at half-maximum (FWHM), indicating the state of molybdenum to be also very similar. This leads to the assumption that a more or less three-dimensional MoO_3 structure is present on TiO_2, whereas on the much larger surface of TiO_2–Al_2O_3 and Al_2O_3 a poorly crystalline two-dimensional network of molybdenum might be present. Under this assumption, the different oxidation states and the discrepancies of the detected FWHM can be explained. Nevertheless, there is no direct experimental proof for this suggestion.

Table 2 shows the FWHM derived from the Mo 3d XPS spectra of the calcined, unsulfided molybdena catalysts. The TiO_2 coverage of the composite support has been varied in order to elucidate the influence on the state of the Mo-species on the surface. As already stated above, the spectra of Mo/TiO_2 reveals the lowest FWHM, whereas the highest values have been obtained for Mo/Al_2O_3. Furthermore, with regard to the composite support, the amount of TiO_2 loaded on the γ-alumina significantly affects the broadening of the peaks in the Mo 3d XPS spectra. The FWHM of

Table 2
FWHM of the XPS peaks corresponding to the Mo $3d_{3/2}$ and $3d_{5/2}$ binding energy for different Mo catalysts

Catalyst	FWHM (eV)	
	Mo $3d_{3/2}$	Mo $3d_{5/2}$
Mo/Al_2O_3	3.33	3.12
Mo/TiO_2–Al_2O_3 (3.54)	2.26	2.39
Mo/TiO_2–Al_2O_3 (6.05)	2.25	2.44
Mo/TiO_2–Al_2O_3 (8.85)	2.16	2.17
Mo/TiO_2–Al_2O_3 (10.20)	2.14	2.24
Mo/TiO_2–Al_2O_3 (13.10)	2.53	2.75
Mo/TiO_2	1.70	1.82

MoO_3 loading: 6 wt%. Values in parentheses correspond to the TiO_2 loadings.

the Mo/TiO_2–Al_2O_3 catalysts fundamentally is increased by higher titania coverages. Nevertheless, no strictly linear correlation has been observed. In particular, this is true for the samples covered with 8.85 and 10.20 wt% TiO_2. Nevertheless, the state of the molybdenum species on the TiO_2–Al_2O_3 composite support can be regarded as a transition state between the Mo/Al_2O_3 and Mo/TiO_2. The broadening of the 3d XPS peaks might be caused by strong interactions between Mo and the support, as well as by structural distortions. TiO_2 loadings of 8.85 and 10.20 wt% provide Mo species which are more similar to the Mo species present on pure TiO_2 supports than to molybdenum supported on Al_2O_3. The fact that TiO_2 loadings of 13.10 wt% lead to larger FWHM of the Mo XPS peaks might be caused by saturation effects while loading the Al_2O_3 surface with TiO_2 and the formation of TiO_2 precipitations. However, within the sensitivity of the experimental techniques used, no TiO_2 clusters have been detected.

After sulfurization, the maxima due to Mo(VI)-species have strongly decreased. The binding energies for crystalline MoS_2 (H) are 233.0 eV ($3d_{3/2}$) and 229.9 eV ($3d_{5/2}$). The spectra of sulfided MoO_3 on the different supports can also be assigned to MoS_2 species, whereas Mo (VI) species are still present. As already obtained for the calcined materials, sulfided Mo/Al_2O_3 (E) and Mo/TiO_2–Al_2O_3 (G) reveal broader binding energy distributions than MoS_2 and Mo/TiO_2 (F). This might be caused by the same reasons as mentioned above. However, the binding energies ($3d_{5/2}$) of the sulfided catalysts increase as follows: Mo/Al_2O_3<Mo/TiO_2–Al_2O_3=Mo/TiO_2. Nevertheless, in agreement with the calcined materials, the spectra of MoS_2 and of sulfided Mo/TiO_2 are very similar with regard to the FWHM of the peaks, indicating the structure to be very similar. As already stated above, and in particular in the case of the Al_2O_3 support, there are still Mo(VI) species present and the sensitivity of the XPS technique used, is not high enough to make any conclusion on the exact structural state of Mo on the surface of the different supports.

Fig. 5 shows the Ni 2p XPS spectra of crystalline NiO (A), Ni–Mo/Al_2O_3 (B), Ni–Mo/TiO_2 (C) and Ni–Mo/TiO_2–Al_2O_3 (D). NiO reveals binding energies of 873.7 eV ($2p_{1/2}$) and 856.1 eV ($2p_{3/2}$), whereas the highest values are detected for Ni–Mo/Al_2O_3 (874.3 and 856.5 eV). Concerning the binding energies of Ni

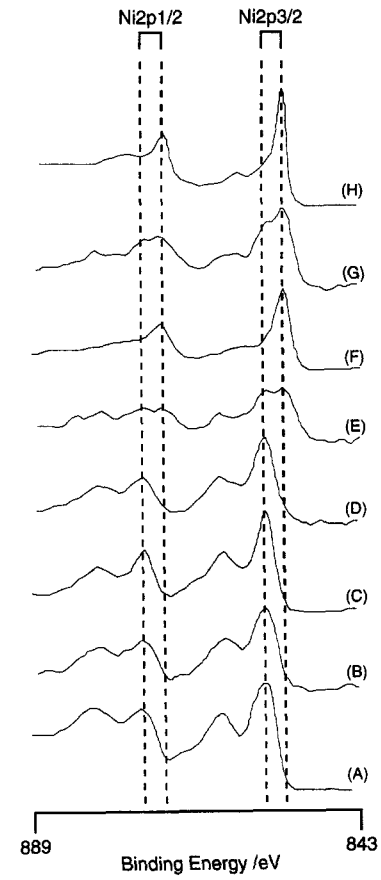

Fig. 5. Ni 2p XPS spectra of the calcined (A, B, C, D), the sulfided (E, F, G) Ni–Mo catalysts: NiO (A), Ni–Mo/Al_2O_3 (B, E), Ni–Mo/TiO_2 (C, F), Ni–Mo/TiO_2–Al_2O_3 (10.0 wt% TiO_2) (D, G) and sulfided NiO (H).

on different supports, not only interactions between Ni and the carrier, but also interactions between nickel and the molybdenum species have to be considered. Nevertheless, and in contrast to the Mo 3d spectra described above, the Ni 2p spectra of the calcined catalysts are very similar with regard to the FWHM of the maxima, indicating the state of NiO on the surface of all catalysts to be very similar to crystalline NiO.

The corresponding XPS spectra of the sulfided materials are also displayed in Fig. 5 (E, F, G, H). Louwers and Prins [39] reported nickel to be present in a Ni_3S_2-like phase after sulfurization. The binding energies of sulfided NiO (H) are 870.9 eV ($2p_{1/2}$) and 853.7 eV ($2p_{3/2}$). Ni–Mo/Al_2O_3 still reveals strong maxima due to NiO species, indicating a significant amount of unsulfided species to be present. The

Table 3
Surface properties of different Mo catalysts as derived from the Mo 3d XPS spectra

Catalyst	S/Mo	$[MoS_2]^a$
Mo/Al_2O_3	1.30	0.63
Mo/TiO_2–Al_2O_3 (3.54)	1.26	0.63
Mo/TiO_2–Al_2O_3 (6.05)	1.47	0.68
Mo/TiO_2–Al_2O_3 (8.85)	1.54	0.71
Mo/TiO_2–Al_2O_3 (10.20)	1.63	0.71
Mo/TiO_2–Al_2O_3 (13.22)	1.65	0.79
Mo/TiO_2	1.74	0.82

Pretreatment: 5% H_2S/95% H_2, 573 K; MoO_3 loading: 6.0 wt%, MoS_2 (S/Mo=2.29). Values in parentheses correspond to the TiO_2 loading (wt%).
[a]$MoS_2/(MoS_2+MoO_3)$.

Table 4
Surface properties of Ni–Mo catalysts according to the Ni 2p XPS spectra

Catalyst	S/Mo	$[MoS_2]^a$	$[Ni_3S_2]^b$
$NiMo/Al_2O_3$	1.51	0.63	0.43
$NiMo/TiO_2$–Al_2O_3 (3.61)	1.69	0.62	0.44
$NiMo/TiO_2$–Al_2O_3 (5.32)	1.79	0.69	0.41
$NiMo/TiO_2$–Al_2O_3 (8.83)	2.06	0.77	0.53
$NiMo/TiO_2$–Al_2O_3 (9.70)	2.03	0.78	0.55
$NiMo/TiO_2$–Al_2O_3 (13.10)	2.04	0.81	0.53
$NiMo/TiO_2$	2.45	0.81	0.77

Pretreatment: 5% H_2S/95% H_2, 573 K; NiO: 3.0 wt%, MoO_3: 6.0 wt%, MoS_2 (S/Mo=2.29). Values in parentheses correspond to the TiO_2 loading (wt%).
[a]$MoS_2/(MoS_2+MoO_3)$.
[b]$Ni_3S_2/(NiO+Ni_3S_2)$.

spectrum of Ni–Mo/TiO_2–Al_2O_3 also exhibits peaks which can be assigned to NiO. Nevertheless, those peaks are much less intense than in the case of Ni–Mo/Al_2O_3. According to these results, NiO can best be transferred to the sulfided species over the TiO_2 support, whereas sulfurization of NiO over the composite TiO_2–Al_2O_3 support is more efficient than over γ-alumina.

The ratios of S(2p)/Mo(3d), $MoS_2/(MoS_2+MoO_3)$, for the different supports are depicted in Table 3. The $MoS_2/(MoS_2+MoO_3)$ ratio has been derived from the normalized XPS peak intensities, using a Gauss–Lorentz profile. To elucidate the influence of the TiO_2 loading on the surface properties of the Mo/TiO_2–Al_2O_3 catalyst, we investigated the $MoS_2/(MoS_2+MoO_3)$ ratio as a function of the TiO_2 loading. The results are also shown in Table 3. Concerning the different supports, the S/Mo ratio clearly increases in the order: Al_2O_3<TiO_2–Al_2O_3<TiO_2. Furthermore, higher TiO_2 loadings also lead to larger S/Mo ratios. Only the composite support coated with 3.54 wt% TiO_2 revealed a lower S/Mo ratio than γ-alumina. Table 3 also indicates that, on the surfaces of all catalysts, not all molybdenum has been sulfided to MoS_2, which is in agreement with the XPS data already discussed.

However, our XPS studies unambiguously reveal that the reducibility from oxidic to sulfidic molybdenum species on the TiO_2–Al_2O_3 composite support is higher than that on the Al_2O_3 support. The possible reasons are the differences in the interactions between Mo species and the different supports. This is in agreement with the different FWHM of the peaks in the Mo XPS spectra, which were strongly dependent on the TiO_2 loading, implying different states of molybdenum. As already stated above, broad peaks in the XPS spectra indicate strong Mo-support interactions, which may lead to lower reducibilities of MoO_3 to MoS_2. Therefore, Mo/TiO_2 provides high transitions to the lower valence state of Mo, whereas Mo species on pure γ-alumina reveal the lowest reducibility during sulfurization.

The S/Mo, $MoS_2/(MoS_2+MoO_3)$ and $Ni_3S_2/(Ni_3S_2+NiO)$ ratios for the corresponding Ni–Mo catalysts are displayed in Table 4. The S/Mo ratio increases in the same order as found for the molybdenum catalysts. However, the Ni–Mo/TiO_2–Al_2O_3 materials with rather high TiO_2 loadings (8.83, 9.70, and 13.10 wt%) exhibit almost the same ratios. This is also true for the $MoS_2/(MoS_2+MoO_3)$ ratio. The ratios obtained for Ni–Mo/TiO_2 and Ni–Mo/TiO_2–Al_2O_3 (13.10 wt%) are equal, the $Ni_3S_2/(Ni_3S_2+NiO)$ ratios obtained for Ni–Mo/Al_2O_3 and Ni–Mo/TiO_2–Al_2O_3 (3.61 wt% TiO_2 and 5.32 wt% TiO_2) are almost the same. With the exception of Ni–Mo/TiO_2–Al_2O_3 (5.32 wt%), the $Ni_3S_2/(Ni_3S_2+NiO)$ ratios for the Ni–Mo catalysts supported on TiO_2–Al_2O_3 are higher compared to those for the γ-alumina supported Ni–Mo catalyst. In particular in the case of the TiO_2–Al_2O_3 composite supports with higher TiO_2 loadings (8.83, 9.70 and 13.10 wt%), the $Ni_3S_2/(Ni_3S_2+NiO)$ ratios are about 25% higher than that obtained for the Al_2O_3 support. The highest $Ni_3S_2/(Ni_3S_2+NiO)$ ratio was found for the pure TiO_2

Table 5
Conversions obtained over Mo catalysts for the HDS of DBT, 4-MDBT and 4,6-DMDBT

Catalyst	Conversion (%)		
	DBT	4-MDBT	4,6-DMDBT
Mo/Al_2O_3	61.04 (0.06)	29.09 (0.12)	6.29 (0.34)
Mo/TiO_2–Al_2O_3 (3.54)[a]	69.76 (0.05)	31.76 (0.13)	16.29 (0.45)
Mo/TiO_2–Al_2O_3 (6.05)[a]	75.12 (0.06)	38.81 (0.13)	19.25 (0.54)
Mo/TiO_2–Al_2O_3 (8.85)[a]	71.38 (0.06)	44.91 (0.15)	28.90 (0.64)
Mo/TiO_2–Al_2O_3 (10.20)[a]	78.39 (0.06)	43.96 (0.16)	34.81 (0.69)
Mo/TiO_2–Al_2O_3 (13.22)[a]	76.02 (0.04)	42.52 (0.13)	22.37 (0.56)
Mo/TiO_2	83.17 (0.06)	46.37 (0.14)	21.12 (0.59)

MoO_3: 6 wt%; pretreatment: 5% H_2S/95% H_2 at 573 K, reaction temperature: 573 K; H_2 pressure: 3 MPa, H_2 flow: 200 cm^3 min^{-1}, LHSV: 12.08–16.07 h^{-1}. Values in parentheses represent the ratio of the CHB/BP derivatives.
( )[a]: TiO_2 (wt%).

support. However, Ni–Mo/TiO_2–Al_2O_3 (13.10 wt% TiO_2) exhibits a slightly lower $Ni_3S_2/(Ni_3S_2+NiO)$ ratio than Ni–Mo/TiO_2–Al_2O_3 with a TiO_2 loading of 9.70 wt%. Furthermore, judged by the results presented in Table 4, and in agreement with the XPS spectra, the NiO species have not been completely sulfided under these conditions. The $Ni_3S_2/(Ni_3S_2+NiO)$ ratios detected for the composite support with rather high amounts of TiO_2 are higher than those of Ni–Mo/Al_2O_3. The fact that the $Ni_3S_2/(Ni_3S_2+NiO)$ ratios did not show a linear increase with increasing TiO_2 loadings may be due to different surface morphologies. Nevertheless, our studies unambiguously reflect sulfurization of the nickel, as well as of molybdenum species, to be more efficient over the composite supports than over Al_2O_3.

3.3. HDS reaction

As already pointed out, the HDS of DBT derivatives leads to the corresponding substituted BP and CHB compounds. The product selectivity mainly depends on the reaction pathway. Prehydrogenation of neighboring phenyl groups leads to an intermediate, and then CHB derivatives are produced (HDS route). In contrast to that, the desulfurization without prehydrogenation (direct desulfurization route) leads to the corresponding BP products.

The conversions obtained at 573 K and a H_2 pressure of 3 MPa, for the HDS reaction of DBT, 4-MDBT and 4,6-DMDBT, over the Mo catalysts under investigation is depicted in Table 5. With regard to DBT, the conversion rate over the different catalysts increases as follows: Mo/Al_2O_3<Mo/TiO_2–Al_2O_3 (3.54–13.22 wt%)<Mo/TiO_2. However, even materials with TiO_2 loadings of only 3.54 wt% titania show higher conversion rates of DBT than Mo supported on pure γ-alumina. In the case of DBT, the CHB/BP ratios of all catalysts are around 0.05. Concerning the conversions of 4-MDBT and 4,6-DMDBT, all catalysts revealed lower conversion rates, because of the lower reactivities of these compounds. However, with regard to 4-MDBT, the ratios of the methyl-substituted CHB/BP ratios detected over the investigated catalysts are very similar, whereas observed conversions are significantly higher over Mo/TiO_2–Al_2O_3 and Mo/TiO_2. Thus, the high catalytic activity for the HDS of 4-MDBT over Mo/TiO_2–Al_2O_3 and Mo/TiO_2 must be due to the direct desulfurization pathway. However, most remarkable is the very high catalytic activity of the TiO_2–Al_2O_3 supported molybdenum, reaching conversions of 34.81% (10.20 wt% TiO_2) for the HDS of 4,6-DMDBT. Over Mo/Al_2O_3, 4,6-DMDBT conversions of only 6.29% are obtained. The high conversions for the HDS of 4,6-DMDBT over Mo/TiO_2–Al_2O_3 can mainly be attributed to the high ratios of corresponding CHB/BP ratios, which become higher than those obtained over Mo/TiO_2 and Mo/Al_2O_3. This implies the hydrodesulfurization route to be more important for the HDS of 4,6-DMDBT over Mo/TiO_2–Al_2O_3 compared to the Al_2O_3 and TiO_2 supported Mo catalysts. As already pointed out above, prehydrogenation of an aromatic ring reduces the steric hindrance by methyl groups during the C–S bond scission and leads to the corresponding CHB derivatives. However, the conversions of 4-MDBT and

Table 6
Conversions obtained over Ni–Mo catalysts for the HDS of DBT, 4-MDBT and 4,6-DMDBT

Catalyst	Conversion (%)		
	DBT	4-MDBT	4,6-DMDBT
$NiMo/Al_2O_3$	93.27 (0.06)	65.50 (0.19)	31.92 (0.72)
$NiMo/TiO_2–Al_2O_3$ (3.54)[a]	93.69 (0.08)	66.37 (0.20)	34.12 (0.72)
$NiMo/TiO_2–Al_2O_3$ (6.05)[a]	93.16 (0.09)	66.05 (0.25)	40.94 (0.72)
$NiMo/TiO_2–Al_2O_3$ (8.83)[a]	93.50 (0.09)	67.45 (0.30)	43.93 (0.79)
$NiMo/TiO_2–Al_2O_3$ (10.30)[a]	93.81 (0.10)	68.75 (0.31)	44.31 (0.83)
$NiMo/TiO_2–Al_2O_3$ (13.10)[a]	93.44 (0.08)	66.74 (0.25)	43.21 (0.76)
$NiMo/TiO_2$	90.51 (0.11)	61.94 (0.35)	39.29 (1.27)

MoO_3: 6 wt%, NiO: 3 wt%; pretreatment: 5% H_2S/95% H_2 at 573 K, reaction temperature: 573 K; H_2 pressure: 3 MPa, H_2 flow: 200 $cm^3\ min^{-1}$; S content: 0.05 wt% in dodecane, LHSV: 24.16–32.14 h^{-1}. Values in parentheses represent the ratio of the CHB/BP derivatives.
( )[a]: TiO_2 wt%.

4,6-DMDBT over $Mo/TiO_2–Al_2O_3$ (13.22 wt% TiO_2) are not as high than those obtained over $Mo/TiO_2–Al_2O_3$ with lower TiO_2 loadings (8.85 and 10.20 wt%).

The conversions of DBT, 4-MDBT and 4,6-DMDBT, as well as the CHB/BP ratios obtained over the corresponding Ni–Mo catalysts are depicted in Table 6. As is already known, nickel enhances the catalytic activity, leading to conversions for DBT above 90% over all materials under investigation. The CHB/BP ratios over $Ni–Mo/TiO_2–Al_2O_3$ and $Ni–Mo/TiO_2$ are higher than those obtained over the molybdenum catalysts. This implies with regard to $Ni–Mo/TiO_2–Al_2O_3$ and $Ni–Mo/TiO_2$ that the HDS route will become more important than over the corresponding Mo catalysts. Concerning the HDS of 4-MDBT and 4,6-DMDBT, the catalytic activity of $Ni–Mo/TiO_2–Al_2O_3$ increases with the amount of TiO_2 loaded on the γ-alumina surface, becoming significantly higher than the activity obtained for $Ni–Mo/TiO_2$. However, over the Ni–Mo catalysts, the highest CHB/BP ratios were obtained for the pure TiO_2 support. The conversions of all DBT derivatives detected over the composite supports with titania loadings of 6.05 wt% and above are higher than those achieved over $Ni–Mo/TiO_2$. For the HDS of 4-MDBT and 4,6-DMDBT, $Ni–Mo/TiO_2–Al_2O_3$ (10.30 wt% TiO_2) showed about 10% higher conversions than $Ni–Mo/TiO_2$, even though the detected CHB/BP ratio is lower over the composite supported catalyst. TiO_2 loadings of 13.10 wt% lead to a decrease of the obtained conversions and the ratio of corresponding CHB/BP derivatives. This is true for all sulfur compounds under investigation. In correspondence to Kabe and co-workers [33], the formation of CHB derivatives from the corresponding BP compounds over Ni-promoted catalysts is not expected to be important at these mild reaction conditions. According to the presented results, Ni promotes the catalytic activity of the composite supported Ni–Mo catalyst more than the catalytic activity of $Ni–Mo/TiO_2$.

To elucidate the influence of the positions of methyl groups on the conversion rate in a mixture of different DBT derivatives, we studied the HDS of a mixture of DBT, 4-MDBT and 4,6-DMDBT (molar ratio: 1/1/1) over Ni–Mo catalysts on the different supports (Al_2O_3, TiO_2 and $TiO_2–Al_2O_3$). In the course of this investigation, we used a $TiO_2–Al_2O_3$ composite support with a rather high titania loading (10 wt%). For comparison, the HDS of a mixture of DBT, 2-MDBT and 2,8-DMDBT (molar ratio: 1/1/1) has been performed under the same reaction conditions. The conversion rates as well as the reaction conditions are depicted in Table 7. With regard to the conversion of the mixture containing DBT, 4-MDBT and 4,6-DMDBT, the activities increase in the order: $Ni–Mo/Al_2O_3$<$Ni–Mo/TiO_2–Al_2O_3$<$Ni–Mo/TiO_2$. This is in contrast to the conversions obtained for the HDS of the different compounds presented in Table 6. Therefore, further studies on $TiO_2–Al_2O_3$ supported Ni–Mo catalysts with different titania loadings will be carried out, to elucidate the influence of the amount of TiO_2 on the catalytic activity under these reaction conditions. However, in particular for the HDS of 4,6-DMDBT,

Table 7
Conversions obtained over Ni–Mo catalysts for the HDS of a mixture of DBT, 2-MDBT and 2,8-DMDBT (B), as well as of a mixture of DBT, 4-MDBT and 4,6-DMDBT (A)

Catalyst	Mixture	Conversion (%)		
		DBT	C1DBT	C2DBT
$NiMo/Al_2O_3$	A	63.3	31.8	9.9
$NiMo/TiO_2$	A	75.6	39.6	17.0
$NiMo/TiO_2$–Al_2O_3[a]	A	67.3	34.6	14.9
$NiMo/Al_2O_3$	B	49.1	67.7	86.4
$NiMo/TiO_2$	B	64.4	78.5	90.9
$NiMo/TiO_2$–Al_2O_3[a]	B	61.3	79.4	91.0

[a]Prepared by CVD method.
MoO_3: 6 wt%, NiO: 3 wt%, TiO_2: 10 wt%; pretreatment: 5% H_2S/95% H_2 at 573 K, reaction temperature: 573 K; H_2 pressure: 3 MPa, H_2 flow: 200 $cm^3\ min^{-1}$, LHSV: 24.16–32.14 h^{-1}. Mixture A: DBT, 4-MDBT, 4,6-DMDBT in dodecane. Mixture B: DBT, 2-MDBT, 2,8-DMDBT in dodecane. C1DBT: 4-MDBT or 2-MDBT, C2DBT: 4,6-DMDBT or 2,8-DMDBT.

the conversions obtained over Ni–Mo/Al_2O_3–TiO_2 and Ni–Mo/TiO_2 are much higher than the conversion detected over the Al_2O_3 supported catalyst. As expected, the conversion for the different sulfur compounds increases as follows: DBT>4-MDBT>4,6-DMDBT. The order of the conversion for DBT in a mixture containing DBT, 2-MDBT and 2,8-DMDBT is as follows: Ni–Mo/Al_2O_3<Ni–Mo/TiO_2–Al_2O_3<Ni–Mo/TiO_2, whereas for 2-MDBT and 2,8-DMDBT the catalytic activity of Ni–Mo/TiO_2–Al_2O_3 is slightly higher (2-MDBT) or almost equal (2,8-DMDBT) to the activity of Ni–Mo/TiO_2. However, the conversion of DBT in a mixture with 2-MDBT and 2,8-DMDBT is lower than in a mixture containing 4-MDBT and 4,6-DMDBT.

This leads to the assumption of a competitive mechanism between these sulfur compounds. The electron density at the sulfur atom is enhanced in the case of all methyl-substituted DBT derivatives. Nevertheless, concerning the direct desulfurization pathway, the steric hindrance retarding the C–S bond occurs only when the methyl groups are at 4 or 4,6 position. However, the conversions of 2-MDBT and 2,8-DMDBT in a mixture with DBT are as follows: 2,8-DMDBT>4-MDBT>DBT. Due to the higher electron density located at the sulfur, the highest conversion over all catalysts under investigation was found for 2,8-DMDBT. The conversion rates obviously reveal the lower catalytic activity of the Al_2O_3 supported catalysts, compared to the TiO_2 and TiO_2–Al_2O_3 supported materials. This is true for all sulfur compounds contained in the two mixtures.

Judged by the detected conversions discussed above, over TiO_2–Al_2O_3 and TiO_2 supported Ni–Mo catalysts, the HDS route is much more important than over the material supported on Al_2O_3. According to Mochida and co-workers [32], the prehydrogenation of an aromatic ring leads to higher reactivities of 4-MDBT and 4,6-DMDBT. This results in comparably high conversions for the HDS of 4-MDBT and 4,6-DMDBT over the molybdenum and Ni–Mo catalysts supported on the TiO_2–Al_2O_3 composite material. In agreement with Kabe and co-workers [33], the reactivity of the sulfur compounds under investigation decreases in the order: 2,8-DMDBT>2-MDBT>DBT>4-MDBT>4,6-DMDBT. This is true for all investigated catalysts. The conversion obtained over Ni–Mo catalysts clearly reflects the role of Ni as a promoter of the catalytic activity of all investigated materials.

4. Conclusion

In order to design a suitable catalyst for the deep HDS of DBT derivatives, we prepared TiO_2–Al_2O_3 supports by CVD.

1. Concerning the preparation of TiO_2–Al_2O_3 composite supports, CVD allows us to coat the surface of alumina with TiO_2 using $TiCl_4$ as precursor for titania, leading to the substitution of Al–OH groups by Al–O–Ti bridges. TiO_2 species are highly dispersed on the alumina surface, preserving a specific surface area comparable to γ-alumina, while the amount of TiO_2 can be varied over a wide range by choosing different deposition times.
2. $Mo(VI)O_3$ species situated on TiO_2–Al_2O_3 composite supports can be transferred much more easily into $Mo(IV)S_2$ by sulfurization and reduction than $Mo(VI)O_3$ species on pure Al_2O_3 support. This is also true for the sulfurization of NiO species.
3. With regard to TiO_2–Al_2O_3 supported Ni–Mo catalysts the prehydrogenation of the DBT derivatives

was very important, resulting in rather high ratios of the corresponding CHB/BP derivatives and to high conversion rates, in particular for the deep HDS of 4-MDBT and 4,6-DMDBT.

4. According to the low CHB/BP ratios obtained over Al_2O_3 supported Mo and Ni–Mo catalysts, the direct desulfurization route is preferred much more strongly than over the corresponding TiO_2–Al_2O_3 materials, leading to significantly lower conversions of 4-MDBT and 4,6-DMDBT.
5. Furthermore, a strong dependence of the catalytic activity as well as of the efficiency of the sulfurization on the amount of TiO_2 loaded on the γ-alumina surface has been observed.

The presented results indicate that the composite TiO_2–Al_2O_3 supports prepared by CVD allow us to overcome the disadvantages of pure TiO_2 supports as described above, providing a very high catalytic activity for the deep HDS of DBT derivatives. Further studies will be performed in order to elucidate the influence of the size of the specific surface area on the deep HDS reaction over the different materials. However, TiO_2–Al_2O_3 supports are suitable candidates to substitute γ-alumina in the industrial deep HDS processes.

References

[1] K.Y.S. Ng, E. Gulari, J. Catal. 95 (1985) 33.
[2] Y. Okamoto, A. Maezawa, T. Imanaka, J. Catal. 120 (1989) 29.
[3] H. Shimada, T. Sato, Y. Yoshimura, J. Hirai, A. Nishijima, Shokubai 27 (1985) 404.
[4] K. Segawa, T. Soeya, D.S. Kim, Chem. Intermediates. 15 (1991) 129.
[5] S. Matsudo, A. Kato, Appl. Catal. 8 (1983) 149.
[6] G. Muralidhar, F.E. Massoth, J. Shabtai, J. Catal. 85 (1984) 44.
[7] A. Spojakina, S. Damyanova, D. Shopov, T. Shokhireva, T. Yurieva, React. Kin. Catal. Lett. 27 (1985) 333.
[8] A. Fernandez, J. Leurer, A.R. Gonzales-Elipe, G. Munuera, H. Knozinger, J. Catal. 112 (1988) 489.
[9] D.S. Kim, Y. Kurusu, I.E. Wachs, F.D. Hartcastle, K. Segawa, J. Catal. 120 (1989) 325.
[10] N. Spanos, H.K. Matralis, C.H. Kordulis, A. Lycourghiotis, J. Catal. 136 (1989) 432.
[11] R.B. Quincy, M. Houalla, A. Proctor, D.M. Hercules, J. Catal. 125 (1990) 214.
[12] J. Ramirez, R. Cuevas, L. Gasque, M. Vrinat, M. Breysse, Appl. Catal. 71 (1991) 351.
[13] A.N. Desikan, L. Huang, S.T. Oyama, J. Chem. Soc. Faraday Trans. 88 (1992) 3357.
[14] G.C. Bond, S.F. Tahir, Appl. Catal. A 105 (1993) 289.
[15] S. Damyanova, A. Spojakina, React. Kinet. Catal. Lett. 51 (1993) 465.
[16] P. Arnoldy, J.A.M. van den Heijkant, G.D. de Bok, J.A. Moulun, J. Catal. 92 (1985) 35.
[17] A. Nishijima, H. Shimada, T. Sato, T. Yoshimura, J. Hiraishi, Polyhedron 5 (1986) 243.
[18] H. Shimada, T. Sato, Y. Yoshimura, J. Hiraishi, A. Nishijima, J. Catal. 120 (1988) 275.
[19] K. Segawa, M. Katsuta, F. Kameda, Catal. Today. 29 (1996) 215.
[20] S. Damyanova, A. Spojakina, K. Jiratova, Appl. Catal. A 125 (1995) 257.
[21] J.B.Mc. Vicker, J.J Ziemiak, J. Catal. 95 (1985) 473.
[22] K. Foger, J.R. Anderson, Appl. Catal. 23 (1986) 139.
[23] A. Stranick, M. Houalla, D.M. Hercules, J. Catal. 125 (1990) 214.
[24] Z. Wei, Q. Xin, X. Guo, Catal. Lett. 15 (1992) 255.
[25] Z. Wei, Q. Xin, X. Guo, E.L. Sham, P. Granga, B. Delmon, Appl. Catal. 63 (1990) 305.
[26] T. Isoda, K. Ma, I. Mochida, Sekiyu Gakkaishi 37(4) (1994) 368.
[27] A. Ishihara, H. Tajima, T. Kabe, Chem. Lett. (1992) 669.
[28] T. Kabe, A. Ishihara, Q. Zhang, H. Tsutsui, H. Tajima, Sekiyu Gakkaishi 36(6) (1993) 467.
[29] T. Kabe, A. Ishihara, M. Nomura, T. Itoh, P. Qi, Chem. Lett. (1991) 2233.
[30] A. Ishihara, T. Itoh, T. Hino, M. Nomura, P. Qi, T. Kabe, J. Catal. 140 (1993) 184.
[31] A. Ishihara, T. Kabe, Ind. Eng. Chem. Res. 32 (1993) 753.
[32] T. Isoda, X. Ma, I. Mochida, Sekiyu Gakkaishi 37(4) (1994) 368.
[33] Q. Zhang, A. Ishihara, T. Kabe, Sekiyu Gakkaishi 39(6) (1996) 410.
[34] T. Kabe, A. Ishihara, H. Tajima, Ind. Eng. Chem. Res. 31 (1992) 1577.
[35] K. Siegbahn, C. Nordling, A. Fahlman, B. Nordberg, K. Hamrin, J. Hedman, G. Johansson, T. Bergmark, S.E. Karlsson, I. Lindgren, B. Lindberg, ESCA Atomic, Molecular and Solid State Structure Studied by Means of Electron Spectroscopy, Nova Acta Regiae Soc. Sci. Upsaliensis, Ser. 20, Almquist and Wiksells Boktryekeri AB, Stockholm, 1967.
[36] R. Gerdil, E.A. Lucken, J. Am. Chem. Soc. 87(2) (1965) 213.
[37] D. Dollimore, G.R. Heal, J. Appl. Chem. 14 (1964) 109.
[38] C.S. Fadley, S.B.M. Hagstrom, M.P. Klein, D.A. Shirley, J. Chem. Phys. 48 (1968) 3779.
[39] S.P.A. Louwers, R. Prins, J. Catal. 133 (1992) 94.